

Communication

Self-Pilot Tone Based Adaptive Threshold RZ-OOK Decision for Free-Space Optical Communications

Peng-Fei Lv and Yan-Qing Hong * 

School of Information Science and Engineering, Shenyang University of Technology, Shenyang 110870, China; 1366798864@smail.sut.edu.cn

* Correspondence: hongy7@sut.edu.cn

Abstract: This paper studies a novel self-pilot tone based adaptive threshold return-to-zero on-off keying (RZ-OOK) decision for free-space optical (FSO) communications. RZ-OOK has the characteristics of impulse series in the spectrum. Therefore, these impulses can be utilized as the pilot tones of the transmitted signal to convey the channel state information (CSI) of FSO links. Then, the CSI signal is extracted using a local oscillator (LO) with the frequencies of the impulse series and low pass filter. Finally, the adaptive threshold decision (ATD) is realized by assigning optimized weight factors into the extracted CSI signal. The proposed adaptive threshold RZ-OOK decision was studied in simulation under various pulse durations of RZ-OOK signal and frequencies of LO. Simulation results demonstrated that RZ-OOK with the proposed impulse tone-extracted CSI signal under optimized weight factor performs close to the conventional ATD under precise CSI knowledge.

Keywords: return-to-zero on-off keying; adaptive threshold decision; self-pilot tone; free-space optical communications

1. Introduction

Thanks to the tremendous advancement of free-space optical (FSO) communication technology contributed by various research institutes, FSO communication has become a potential technique for 5G+ wireless networks to support high speed and secure data link services [1]. However, the propagated laser beam is sensitive to atmospheric turbulence, which has the character of atmospheric refringence variation [2]. Therefore, numerous studies on adaptive optics, diversity, optical amplifier, polarization shift keying modulation, differential phase shift keying, coherent detection, and adaptive threshold decision (ATD) have been carried out to overcome the issues caused by atmospheric turbulence in order to facilitate the commercialization of FSO communication system [2,3].

ATD technique is widely adopted in intensity modulation and direct detection (IM/DD) FSO communication system, and the decision thresholds of the received signal are determined symbol-by-symbol according to the channel state information (CSI) [4]. Therefore, some studies have been conducted to acquire the knowledge of CSI. Pilot symbols were utilized to convey the required knowledge of CSI by periodically adding the redundant symbols in the stage of signal modulation [5]. However, the code rate is reduced by inserted redundant symbols. Pilot tones were applied to carry the knowledge of CSI by inserting supplemental tones [6,7]. Nonetheless, the procedure of pilot tone insertion increases the system complexity. Closely spaced pilot wavelengths were introduced to deliver the channel information due to a high turbulence channel correlation between signal and pilot wavelength channels [8]. However, it is a waste of wavelength resources and impossible for wavelength division multiplexing (WDM) FSO systems. Low pass filter (LPF) was used after photo detection to extract the low frequency CSI parts out from the received signal [9]. However, the LPF extracted signal contains both CSI and signal components.

In the FSO channel, atmospheric turbulence, atmospheric absorption, and scattering lead to a dramatic optical power loss as to the transmitted signal [10]. Thus, optical



Citation: Lv, P.-F.; Hong, Y.-Q. Self-Pilot Tone Based Adaptive Threshold RZ-OOK Decision for Free-Space Optical Communications. *Photonics* **2023**, *10*, 714. <https://doi.org/10.3390/photonics10070714>

Received: 6 May 2023
Revised: 15 June 2023
Accepted: 19 June 2023
Published: 22 June 2023



Copyright: © 2023 by the authors. Licensee MDPI, Basel, Switzerland. This article is an open access article distributed under the terms and conditions of the Creative Commons Attribution (CC BY) license (<https://creativecommons.org/licenses/by/4.0/>).

amplifier erbium-doped fiber amplifier (EDFA), semiconductor optical amplifier, and Raman amplifier are deployed to enhance the transmitted optical power. Out of three types of amplifier, EDFA is popular in the FSO system due to the advantages of low noise figure and large optical gains [11,12]. EDFA has the physic characteristics of average power limitation at the same time. Therefore, the pulse width of the modulated signal symbol is adjusted to alter the peak power of the transmitted signal according to the link distance and weather conditions [13,14]. With regard to the on-off-keying (OOK) signal transmission in average power-limited EDFA-applied FSO communication system, return-to-zero OOK (RZ-OOK) modulation is more competitive than non-return-to-zero (NRZ) OOK modulation in the aspect of peak pulse power generation via the pulse duration variation. Furthermore, RZ-OOK spectrum has the features of impulse series at an integral multiple of data rate [15]. Thus, these impulse series can be utilized as the pilot tones to deliver the CSI knowledge of the turbulence channel. Therefore, it is preferable to research an alternative approach to estimate the CSI of the turbulence channel taking advantage of RZ-OOK spectrum features in FSO communication systems.

In this study, we propose a self-pilot tone based adaptive threshold RZ-OOK decision for FSO communications. Based on the impulse series features of RZ-OOK spectrum, the CSI of FSO channel is obtained by applying local oscillator (LO) with the same frequencies of the impulse series of RZ-OOK spectrum and LPF. The weight factor is added to the extracted CSI signal in order to improve the power of the CSI signal. The accuracy of CSI estimation is discussed in the case of RZ-OOK with different pulse durations and LO with various frequencies. The proposed technique was investigated in simulation under various FSO channels. Simulation results showed that the bit-error rate (BER) performance of the proposed RZ-OOK with ATD using estimated CSI knowledge is similar to the ATD under precise CSI.

2. Operation Principle

Figure 1 shows the block diagram of the proposed RZ-OOK detection with ATD. RZ-OOK signal with the feature of impulse series in the spectrum is directly modulated into 1550 nm LD. Optical RZ-OOK signal is subjected to the distortion from the atmospheric turbulence channel, i.e., optical power loss and phase distortion of laser beam wave-front [2]. Optical power loss is originated from the atmospheric absorption and scattering caused by atmospheric particles, and it can be compensated by optical amplifier, mainly EDFA, deployed in the transmitter or receiver ends. As to the wave-front phase distortion, the received signal intensity fluctuation caused by the variation of temperature and pressure of atmosphere is the critical issues of FSO system performance degradation [3]. The strength of signal intensity I fluctuation is represented using scintillation index σ_I^2 , and σ_I^2 is given by

$$\sigma_I^2 = \langle I^2 \rangle / \langle I \rangle^2 - 1, \tag{1}$$

where $\langle \cdot \rangle$ is the ensemble average, and a larger σ_I^2 value generates higher degree of intensity fluctuation [6]. The optical RZ-OOK signal is detected using PD to realize an optical to electrical conversion, and the electrical signal after PD $r(t)$ is represented by

$$r(t) = I(t)s(t) + n(t), \tag{2}$$

where $s(t)$ is the transmitted RZ-OOK signal, and $n(t)$ is the average noise power composed of PD and solar noises. Analog signal $r(t)$ is transformed into digital signal $r[k]$ by ADC process. The output signal of ADC is divided into two branches. The upper branch is used to deliver the RZ-OOK signal, and the lower branch is applied to estimate the CSI knowledge. The delay is added into upper branch for the sake of synchronization matching between upper and lower branches. The LO is added into the lower branch, and the

frequencies of LO f_{LO} are configured as the frequencies of impulse series of RZ-OOK spectrum. The signal after LO $c[k]$ is given by

$$c[k] = r[k] \cos(2\pi f_{LO}t). \tag{3}$$

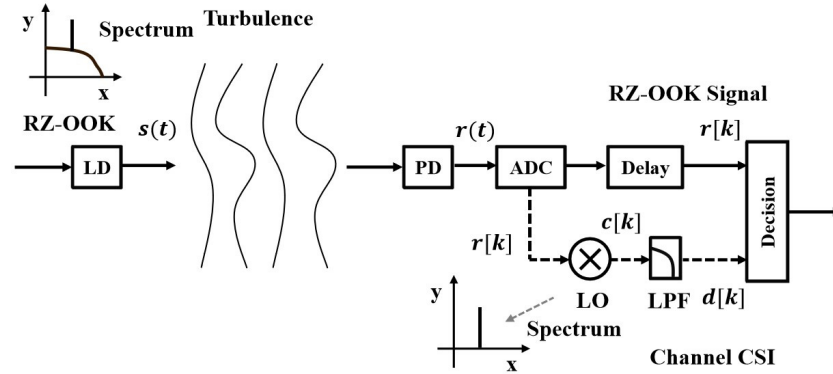


Figure 1. Block diagram of the proposed RZ-OOK detection with ATD. LD: laser diode; PD: photodiode; ADC: analog-to-digital conversion; LO: local oscillator; LPF: low pass filter.

LPF is deployed after LO, and the CSI signal $d[k]$ is extracted by this low pass filtering due to the low frequency characteristics of atmospheric turbulence effect [6]. The weight factor is assigned to $d[k]$, and it is adjusted in the circumstance of different pulse durations and data rates of RZ-OOK and various LO frequencies. Weight factor added $d[k]$ is used as decision thresholds of $r[k]$ signal in the upper branch. The weight factor can be calculated by comparing the maximum signal intensity between RZ-OOK and $d[k]$ at the initial stage of communication. Finally, ATD is achieved for the RZ-OOK transmission by the assistance of impulse tones of RZ-OOK, LO, and LPF. Furthermore, a real-time processing is available for this ATD method. The BER performance is discussed to evaluate the performance of the proposed technique, and the BER is calculated by

$$BER = \int_0^\infty f(r)Q\left(r/\sqrt{2n}\right)dr, \tag{4}$$

$f(r)$ is the probability density function (PDF) of r , and $Q(\cdot)$ is the Q-function [16]. Furthermore, the average signal-to-noise ratio (SNR) is adopted in this work due to the intensity variation of the received RZ-OOK signal, and it is given by

$$SNR = E[I]^2/n, \tag{5}$$

where $E[\cdot]$ is the expected average operation [17].

3. Simulations and Results

We evaluated the proposed adaptive threshold RZ-OOK decision in simulation. The atmospheric turbulence effect was accommodated using the modeled turbulence channel with the properties of intensity variation, low frequency, and lognormal distribution [6,9,10]. The turbulence channels at σ_I^2 of 0.1 and 0.4 were adopted in this simulation. RZ-OOK signal with different pulse durations were introduced, i.e., 75%, 50%, and 25% pulse duration. The frequencies of LO were adjusted to match the frequencies of the impulse series of RZ-OOK spectrum. The RZ-OOK signal with data rate of 100 Mb/s was used in discussion.

Figure 2 illustrates the spectrum of RZ-OOK signal at 75%, 50%, and 25% pulse durations. RZ-OOK signal with lower pulse duration requires a larger spectrum in signal modulation compared to NRZ-OOK due to a narrow pulse width. The impulse series were observed at the spectrum of RZ-OOK signal under different pulse durations. The frequencies of impulse series are an integral multiple of data rate. Furthermore, RZ-OOK

signal with different pulse durations have a same impulse response in the spectrum except for RZ-OOK at a pulse duration of 50%. Since the second order of impulse overlaps with the required spectrum of RZ-OOK at pulse duration of 50%. The frequencies of LO are determined by the frequencies of impulse series. Thus, LO can be simply set to a fixed frequency under various pulse durations of RZ-OOK in the case of certain data rate. Figure 3 shows the frequencies of LO at data rate of 100 Mb/s, and it is used in the following CSI estimation procedure.

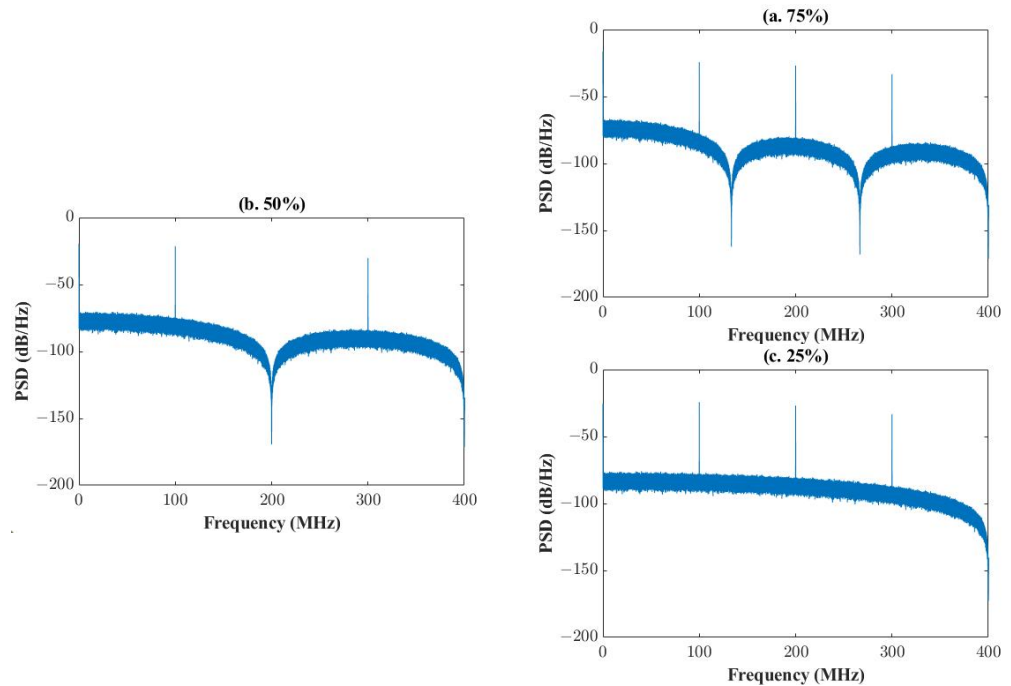


Figure 2. Spectrum of RZ-OOK signal under different pulse durations. (a) 75%, (b) 50%, and (c) 25% pulse durations. PSD: power spectrum density.

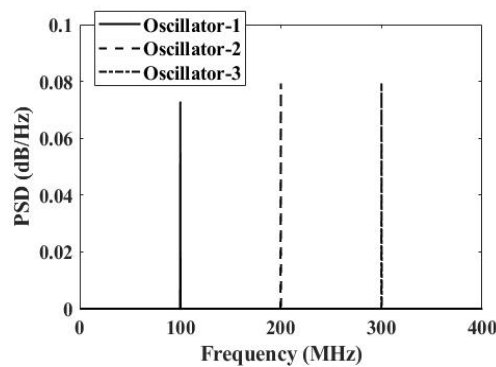


Figure 3. Frequencies of LO at data rate of 100 Mb/s. PSD: power spectrum density.

Figure 4 shows the extracted CSI signal under different frequencies of LO at the turbulence channel with σ_I^2 of 0.1. The cutoff frequency of LPF was set to 100 KHz for the sake of sufficient CSI components filtering. RZ-OOK signal with the pulse duration of 75% was analyzed. Figure 4a demonstrates the precise CSI knowledge of the turbulence channel at σ_I^2 of 0.1, and time-varying RZ-OOK signal intensity variation was observed. Figure 4b illustrates the CSI signal obtained from the first impulse tone of RZ-OOK spectrum using LO frequency of 100 MHz. The correlation coefficient between the estimated CSI and precise CSI signals was 0.9347. Therefore, it can be used as thresholds of RZ-OOK in the ATD process. However, the intensity of the estimated CSI signal is lower than the precise CSI signal. Thus, a weight factor is assigned into the estimated CSI signal. Furthermore, the

weight factor is dependent on the frequency of LO, data rate of RZ-OOK, and pulse duration of RZ-OOK. In this work, the weight factor is calculated and optimized by comparing the maximum signal intensity between RZ-OOK and extracted CSI. Figure 4c,d depict the CSI signal separated from the second and third impulse tones of RZ-OOK spectrum, respectively. LO frequencies of 200 MHz and 300 MHz were applied in the CSI estimation process. The correlation coefficient between the second impulse tone-estimated CSI and precise CSI signals was 0.9347 as well, and the same correlation coefficient was obtained in the case of the third impulse tone application. However, the amplitude of the estimated CSI signal was decreased using higher order impulse tones. Therefore, the weight factors of the estimated CSI signal need to be increased to have an accurate decision threshold. Figures 5 and 6 show the CSI estimation of RZ-OOK signal with the pulse durations of 50% and 25% under different frequencies of LO at σ_I^2 of 0.1. The similar degree of correlation coefficient was achieved compared to RZ-OOK signal with the pulse durations of 75%. The variation of the estimated CSI signal amplitude was observed under different pulse durations and LO frequencies. Consequently, the CSI knowledge of ATD can be acquired from the impulse series of RZ-OOK spectrum and LO with optimized weight factors.

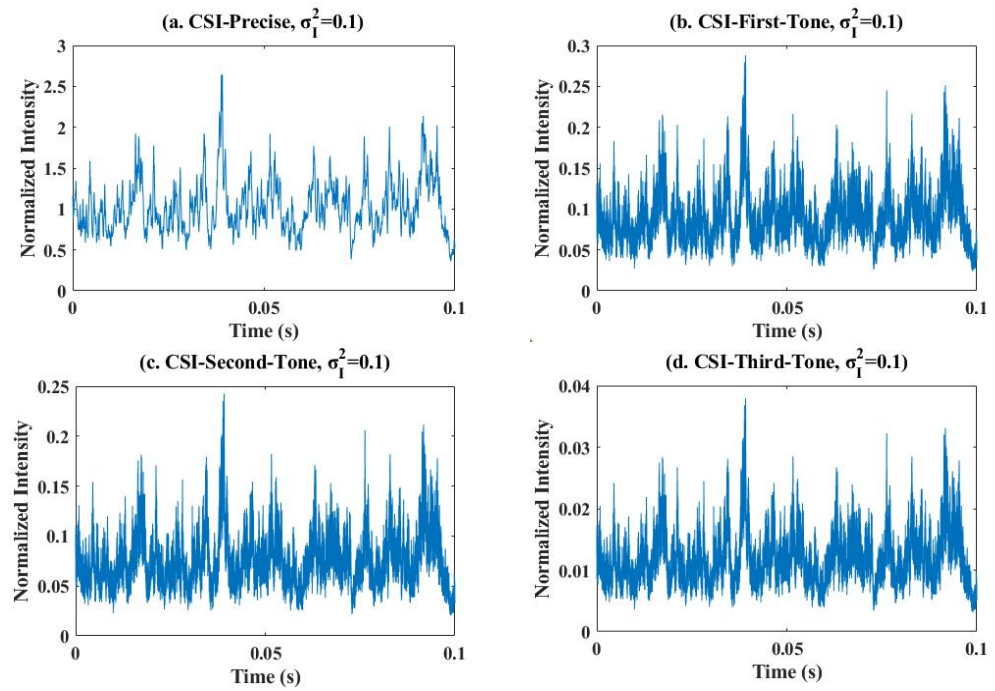


Figure 4. Extracted CSI signal under different frequencies of LO at σ_I^2 of 0.1 and RZ-OOK signal with pulse duration of 75%. (a) Precise CSI, (b) CSI estimation from first impulse tone of RZ-OOK spectrum using LO frequency of 100 MHz, (c) CSI estimation from second impulse tone of RZ-OOK spectrum using LO frequency of 200 MHz, and (d) CSI estimation from the third impulse tone of RZ-OOK spectrum using LO frequency of 300 MHz.

Figure 7 illustrates BER performance of the proposed ATD under the circumstance of RZ-OOK signal with pulse duration of 75% at the turbulence channel with σ_I^2 of 0.1 and 0.4. The BER performance of the proposed ATD was discussed in the case of CSI signal extraction from the first, second, and third impulse tones of RZ-OOK spectrum. The weight factors were optimized according to the results from Figure 4. Furthermore, the BERs of the proposed ATD were compared to the proposed ATD without weight factor and conventional ATD with a precise CSI knowledge in the context of various average SNRs. It is obvious that the BER curves of the proposed ATD with CSI knowledge estimation from different impulse tones of RZ-OOK spectrum were improved compared to the proposed ATD without weight factor, and they were close to the BER curves of conventional ATD. Furthermore, the estimated CSI signal have the same weight factor under σ_I^2 of 0.1 and 0.4.

The BER performance of adaptive RZ-OOK decision was studied under RZ-OOK signal with pulse duration of 50% and 25% as well. Figure 8 shows that the BER curves of ATD in the context of RZ-OOK signal with pulse duration of 50% and 25% were approximate to the curves of conventional ATD as well. Consequently, the proposed adaptive threshold RZ-OOK signal decision was realized under the assistance of impulses of RZ-OOK spectrum, LO, LPF, and optimized weight factors.

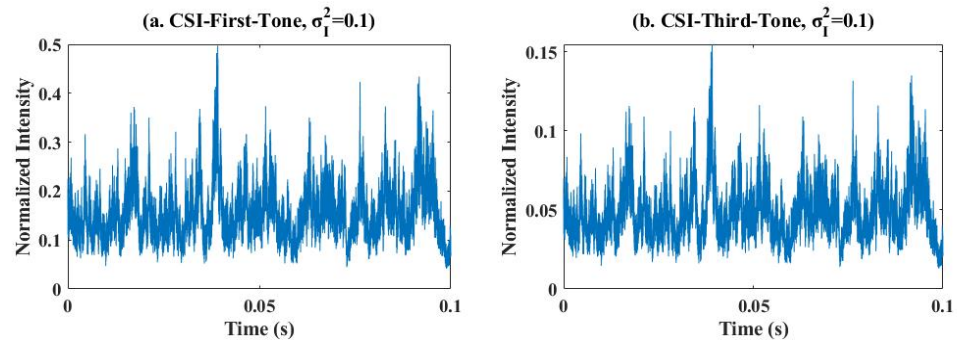


Figure 5. Extracted CSI signal under different frequencies of LO at σ_1^2 of 0.1 and RZ-OOK signal pulse duration of 50%. (a) CSI estimation from first impulse tone of RZ-OOK spectrum using LO frequency of 100 MHz, and (b) CSI estimation from the third impulse tone of RZ-OOK spectrum using LO frequency of 300 MHz.

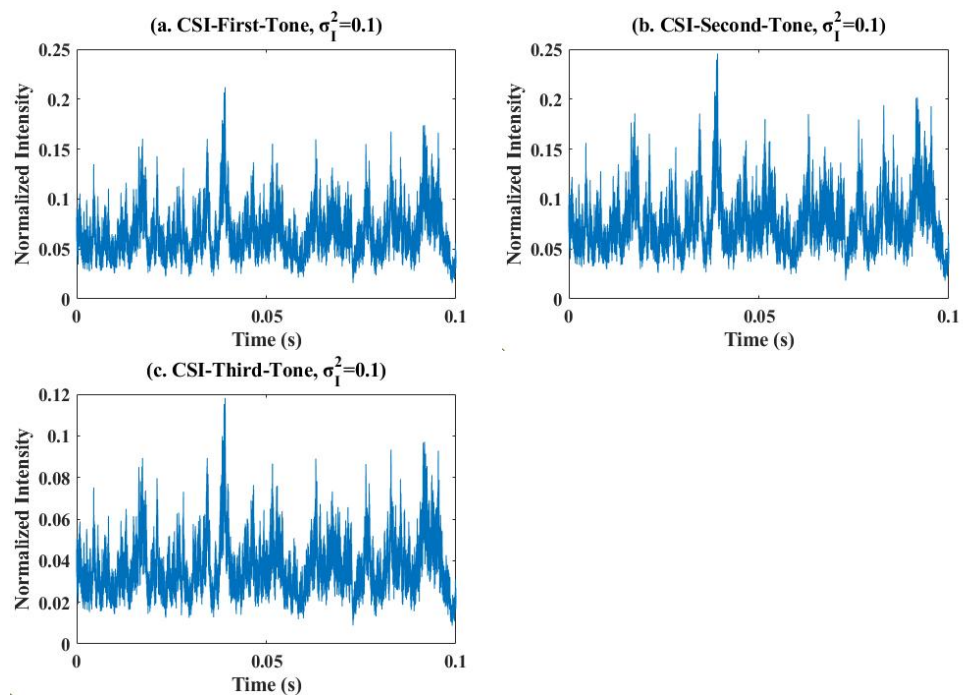


Figure 6. Extracted CSI signal under different frequencies of LO at σ_1^2 of 0.1 and RZ-OOK signal pulse duration of 25%. (a) CSI estimation from first impulse tone of RZ-OOK spectrum using LO frequency of 100 MHz, (b) CSI estimation from second impulse tone of RZ-OOK spectrum using LO frequency of 200 MHz, and (c) CSI estimation from the third impulse tone of RZ-OOK spectrum using LO frequency of 300 MHz.

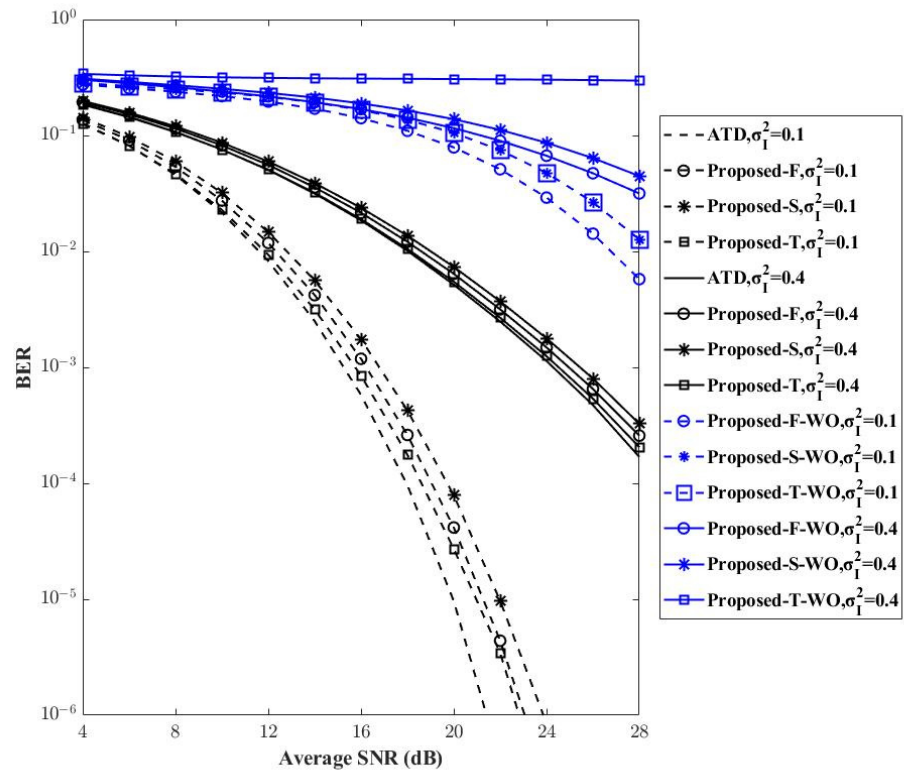


Figure 7. BER performance of the proposed ATD in the context of RZ-OOK signal with pulse duration of 75% at σ_1^2 of 0.1 and 0.4. Proposed-F: proposed ATD with CSI estimation from the first impulse tone; Proposed-S: proposed ATD with CSI estimation from the second impulse tone; Proposed-T: proposed ATD with CSI estimation from the third impulse tone; Proposed-F-WO: Proposed-F without weight factor; Proposed-S-WO: Proposed-S without weight factor; Proposed-T-WO: Proposed-T without weight factor.

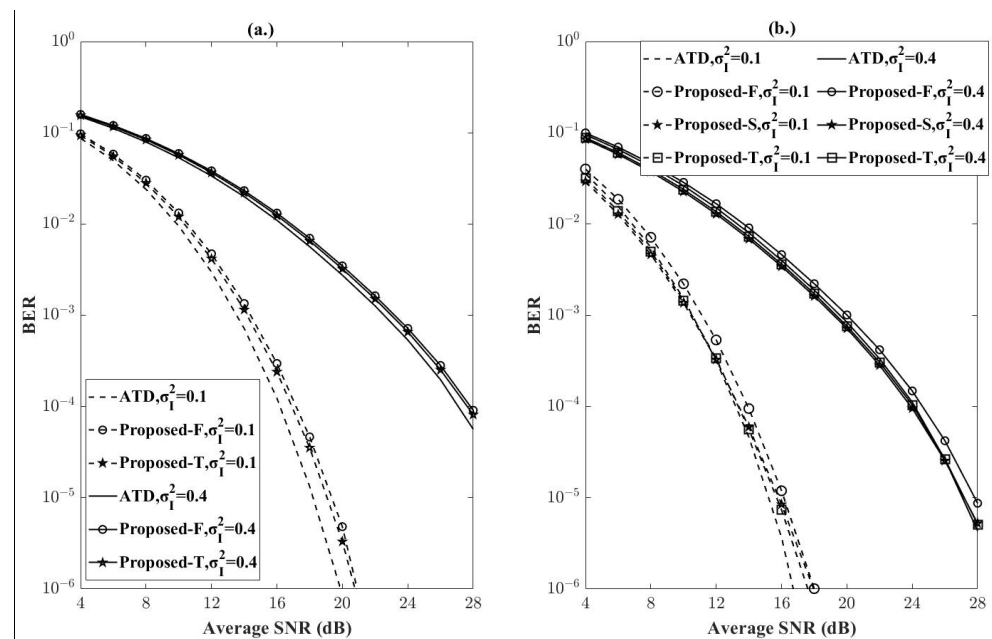


Figure 8. BER performance of the proposed ATD under RZ-OOK signal with the pulse durations of (a) 50%, (b) 25%, at σ_1^2 of 0.1 and 0.4.

4. Conclusions

In summary, we investigated a self-pilot tone based adaptive threshold RZ-OOK decision for FSO communication links. The CSI signal was extracted under the assistance of impulse tones of RZ-OOK spectrum, LO, LPF, and optimized weight factors. Furthermore, the CSI signal fetching process was analyzed in the context of various pulse durations of RZ-OOK and frequencies of LO. The BER performance of the proposed ATD was compared to the conventional ATD under precise CSI knowledge in simulation. Simulation results illustrated that the proposed technique performed close to the conventional ATD. Therefore, it is a highly feasible alternative approach to extract CSI knowledge in FSO systems.

Author Contributions: Conceptualization, Y.-Q.H.; data curation, P.-F.L. and Y.-Q.H.; formal analysis, Y.-Q.H.; project administration, Y.-Q.H.; writing—original draft, P.-F.L. and Y.-Q.H.; writing—review and editing, Y.-Q.H. All authors have read and agreed to the published version of the manuscript.

Funding: This research received no external funding.

Institutional Review Board Statement: Not applicable.

Informed Consent Statement: Not applicable.

Data Availability Statement: Not applicable.

Conflicts of Interest: The authors declare no conflict of interest.

References

1. Alzenad, M.; Shakir, M.Z.; Yanikomeroğlu, H.; Alouini, M.S. FSO-based vertical backhaul/fronthaul framework for 5G+ wireless networks. *IEEE Commun. Mag.* **2018**, *56*, 218–224. [[CrossRef](#)]
2. Hamza, A.S.; Deogun, J.S.; Alexander, D.R. Classification framework for free space optical communication links and systems. *IEEE Commun. Surv. Tutor.* **2019**, *21*, 1346–1382. [[CrossRef](#)]
3. Kaushal, H.; Kaddoum, G. Optical communication in space: Challenges and mitigation techniques. *IEEE Commun. Surv. Tutor.* **2017**, *19*, 57–96. [[CrossRef](#)]
4. Tycz, M.; Fitzmaurice, M.W.; Premo, D.A. Optical communication system performance with tracking error induced signal fading. *IEEE Trans. Commun.* **1973**, *21*, 1069–1072. [[CrossRef](#)]
5. Zhu, X.; Kahn, J.M.; Wang, J. Mitigation of turbulence-induced scintillation noise in free-space optical links using temporal-domain detection techniques. *IEEE Photonics Technol. Lett.* **2003**, *15*, 623–625.
6. Choi, I.Y.; Shin, W.H.; Han, S.K. CSI estimation with pilot tone for scintillation effects mitigation on satellite optical communication. *Opt. Commun.* **2019**, *435*, 88–92. [[CrossRef](#)]
7. Zhang, R.; Hu, N.; Zhou, H.; Zou, K.; Su, X.; Zhou, Y.; Song, H.; Pang, K.; Song, H.; Minoofar, A.; et al. Turbulence-resilient pilot-assisted self-coherent free-space optical communications using automatic optoelectronic mixing of many modes. *Nat. Photon.* **2021**, *15*, 743–750. [[CrossRef](#)]
8. Grant, K.J.; Corbett, K.A.; Clare, B.A. Dual wavelength free space optical communications. In Proceedings of the Conference on Lasers and Electro-Optics, Technical Digest (CD), Baltimore, MD, USA, 22–27 May 2005. paper CTuG3.
9. Ding, S.L.; Zhang, J.K.; Dang, A.H. Adaptive threshold decision for on-off keying transmission systems in atmospheric turbulence. *Opt. Express* **2017**, *25*, 24425–24436. [[CrossRef](#)] [[PubMed](#)]
10. Yoshisada, K.; Morio, T.; Yoshihisa, T.; Hideki, T. The uplink data received by OICETS. *J. Natl. Inst. Inf. Commun. Technol.* **2012**, *59*, 117–123.
11. Wang, Y.; Feng, Y.; Ma, Y.; Chang, Z.; Peng, W.; Sun, Y.; Gao, Q.; Zhu, R.; Tang, C. 2.5 kW narrow linewidth linearly polarized all-fiber MOPA with cascaded phase-modulation to suppress SBS induced self-pulsing. *IEEE Photonics J.* **2020**, *99*, 1502815. [[CrossRef](#)]
12. Engin, D.; Litvinovitch, S.; Gilman, C.; Cao, H.; Wysocki, T.; McIntosh, B.; Rudd, J.; Hqang, J.; Pachowicz, D.; Pettrilo, K.L.; et al. 50 W, 1.5 μm , 8 WDM (25 nm) channels PPM Downlink Tx for Deep Space Lasercom. In Proceedings of the Conference on Free-Space Laser Communications, Online, 6–12 March 2021.
13. Caplan, D.O.; Carney, J.J.; Fitzgerald, J.J.; Gaschits, I.; Kaminsky, R.; Lund, G.; Hamilton, S.A.; Magliocco, R.J.; Murphy, J.; Rao, H.G.; et al. Multi-rate DPSK optical transceivers for free-space applications. In Proceedings of the Free-Space Laser Communication and Atmospheric Propagation XXVI, San Francisco, CA, USA, 1–6 February 2014.
14. Shin, W.H.; Lee, J.W.; Ha, I.H.; Han, S.K. Data rate enhancement of free space optical communication using pulse positioned differential phase shift keying. *Opt. Express* **2021**, *29*, 26039–26047. [[CrossRef](#)] [[PubMed](#)]
15. Ezra, I.; Joseph, M.K. Power Spectra of Return-to-Zero Optical Signals. *J. Lightwave Technol.* **2006**, *24*, 1610–1618.

16. Navidpour, S.; Uysal, M.; Kavehrad, M. BER Performance of Free-Space Optical Transmission with Spatial Diversity. *IEEE Trans. Wirel. Commun.* **2007**, *6*, 2813–2819. [[CrossRef](#)]
17. Riediger, M.; Schober, R.; Lampe, L. Fast multiple-symbol detection for free-space optical communications. *IEEE Trans. Commun.* **2009**, *57*, 1119–1128. [[CrossRef](#)]

Disclaimer/Publisher’s Note: The statements, opinions and data contained in all publications are solely those of the individual author(s) and contributor(s) and not of MDPI and/or the editor(s). MDPI and/or the editor(s) disclaim responsibility for any injury to people or property resulting from any ideas, methods, instructions or products referred to in the content.